

A universal nutrient application strategy for the bioremediation of oil-polluted beaches

Hailong Li ^a, Qinghong Zhao ^a, Michel C. Boufadel ^{a,*}, Albert D. Venosa ^b

^a Department of Civil and Environment Engineering, Temple University, 1947 N. 12th Street, Philadelphia, PA 19122, USA

^b National Risk Management Research Laboratory, US EPA, Cincinnati, OH, USA

Abstract

Biostimulation by nutrient application is a viable technology for restoring oil-contaminated beaches. Maximizing the nutrient residence time is key for achieving a rapid cost-effective cleanup. We considered the nutrient injection strategy through a perforated pipe at the high tide line and we simulated numerically beach hydraulics, which allowed us to estimate the optimal injection flow rate of nutrient solution. Our results indicate that the optimal application is one that starts following the falling high tide and lasts for half tidal cycle. The saturated wet-front of the nutrient solution on the beach surface would move seaward with the same speed of the falling tide keeping a constant distance with the tide line. The numerical results were generalized to beaches of wide ranges of hydraulic and tidal properties using a novel dimensionless formulation for water flow and solute transport in porous media. Nomographs were presented to provide the flow rate based on four parameters: The beach slope and hydraulic conductivity, and tidal amplitude and period.

© 2007 Elsevier Ltd. All rights reserved.

Keywords: Nutrient injection; Oil-polluted beaches; Biostimulation; Bioremediation; Numerical simulation; Optimal strategy; Seawater–freshwater circulation; Dimensionless model

1. Introduction

Oil contamination of coastal areas from offshore spills usually occurs in the intertidal zone of beaches (the beach section between the low tide and the high tide) and occupies, in most situations, the top 25 cm of soil. Mechanical removal of the oil is essential, but unfortunately, cannot achieve 100% removal, and some of the oil remains entrapped in the beach matrix. For this reason, bioremediation (e.g., Merlin et al., 1995; Venosa et al., 1996; Wrenn et al., 2006) of polluted beaches is typically recommended as a follow up treatment strategy. The approach relies on the fact that indigenous microorganism are capable of degrading (oxidizing) the oil provided favorable environmental conditions exist. In particular, the presence of

dissolved oxygen and nutrients, such as phosphate and nitrate, is essential. Dissolved oxygen is commonly present in the interstitial water of beaches, and if it is not, then bioremediation becomes too costly, and thus might not be the best strategy to adopt. However, nutrients can lack on certain beaches, and thus need to be supplied to the bioremediation zone (polluted zone).

Bioremediation studies in the lab and field have demonstrated that nitrogen concentrations ranging from 2.0 to 10.0 mg/L are sufficient for near-maximum growth of hydrocarbon-degrading microorganisms (e.g., Venosa et al., 1996; Boufadel et al., 1999d; Wrenn et al., 2006). The effectiveness of biostimulation depends on prolonged contact between the added nutrients and the oil within the bioremediation zone. Thus, maximizing the residence time of nutrients in this zone is key, and it requires accounting for the factors affecting the transport of dissolved nutrients within the beach matrix. (Slow-release nutrients rely on dissolution in the interstitial water prior to uptake by microorganisms).

* Corresponding author. Tel.: +1 215 204 7871; fax: +1 215 204 4696.

E-mail addresses: hailong@graduate.hku.hk (H. Li), qinghong@temple.edu (Q. Zhao), boufadel@temple.edu (M.C. Boufadel), Venosa.Albert@epamail.epa.gov (A.D. Venosa).

Previous studies indicated that water flow (and subsequently the transport of dissolved nutrient) in a beach is driven by a combination of three main factors: (i) tidal action (Wrenn et al., 1997; Boufadel, 1998; Boufadel et al., 2006), (ii) the presence of freshwater in a marine (saltwater) environment (Boufadel, 2000) and the resulting buoyancy currents, and (iii) wave action (Asservatham et al., 1993; Boufadel et al., in press). The present work accounts only for the first two factors (tide and buoyancy), and presents a nutrient application strategy that is suitable for a wide range of beaches.

In this paper, all the dimensional terms will be marked with a superscript “*”. Any term without the superscript “*” is dimensionless. A list of notations is given in Appendix 1.

2. Application strategy for nutrient

There are two nutrient application strategies that have been considered in the scientific literature. They are: (1) Spraying the nutrient solution onto the beach surface at low tide (using sprinklers), as conducted by Venosa et al. (1996) in their study of a planned oil spill on a Delaware beach, and (2) digging a trench at the high tide line, and applying the solution through a perforated tube during falling tides. This strategy was proposed by Wise et al. (1994a), and it relies on assumed upwelling of nutrients to the bioremediation by freshwater propagating seaward in the beach. The first strategy ensures complete coverage of the bioremediation zone, but it is costly, requiring placing many poles to hold the sprinklers higher than the water level during high tide. In addition, sprinklers tend to jam or clog due to exposure to the abrasive saltwater environment. In the study conducted by Venosa et al. (1996), the staff was dispatching the sprinklers at low tide, conducting the application, and then removing them immediately, a labor-intensive process that is cost prohibitive for a large-scale area. The second strategy was not tested in a field application, but it could be costly if one were to dig trenches in beaches. In addition, the adopted conceptual model of freshwater/saltwater interaction in Wise et al. (1994a) is only appropriate for large-scale dynamics at the scale of aquifers; the model predicts that freshwater is always floating on a saltwater wedge prior to exiting to sea. However, studies at the beach-scale indicated an inverted salinity distribution in the beach, whereby high salinity water overtops low salinity water in the intertidal zone (Millham and Howes, 1994; Wrenn et al., 1997; Boufadel, 1998; Portnoy et al., 1998; Robinson and Gallagher, 1999; Uchiyama et al., 2000; Boufadel, 2000). Thus, the strategy proposed by Wise et al. (1994a) might not be successful.

We propose to apply the nutrients from a perforated pipe placed above the beach surface at the high tide line parallel to the shoreline (Fig. 1). This seems to be the least labor-intensive strategy. Because most of the nutrient in the bioremediation zone will be washed out at the next high

tide, nutrient application should begin immediately after the high tide in order to maximize the residence time of nutrient in the beach.

Our initial inclination was to attempt to saturate the beach with the nutrient solution relying on groundwater flow propagating first downward to the water table and later seaward. This was found to be untenable, because the groundwater seaward propagation of the applied plume was in many situations much slower than the seaward motion of the tide line (intersection of the tide with the beach surface). Our attention was then shifted on using surface runoff of the injected solution as follows: Apply the nutrient solution at a high enough rate to cause “critical” ponding condition on the beach and the seaward runoff of the solution. Here the “critical” ponding condition means that the depth of the ponding nutrient solution on the beach surface is zero (critical) and the pores of the beach surface within the injection area are completely filled with water. Such runoff would percolate into the beach seaward of the application location. If the applied flow is too large, the nutrient runoff would reach the tide line and be washed to sea, which constitutes an inefficient application. Thus, the applied flow needs to be large enough and to vary with time to allow the runoff to fill the beach as soon as the tide falls, because the goal is to maximize the residence time of the nutrients in the beach prior to the rising tide. We elected to have the runoff moving on the beach surface at the same speed of the falling tide (such speed varies with time). The reverse engineering problem was to select the injection flow based on beach and tidal properties. The results are generalized to various beach and tide conditions using a novel dimensionless formulation for water and solute transport in porous media (Boufadel et al., 1999a; Boufadel, 2000). The final results are the variation of the injection flow as function of time and they are presented in form of nomographs requiring the user to input only four parameters (Fig. 1): the beach slope $s_b^* (= \tan \theta)$ [–], the beach soil hydraulic conductivity K_0^* [LT^{-1}] (the beach is assumed to be homogeneous and isotropic), and the tidal amplitude A^* [L] and period T^* [T].

The assumption of homogeneity and isotropy might not be realistic for some beaches, and in those cases the current study would be used as a first try to be followed by an improved design based on numerical simulations or observations.

3. Methods

We define here *the nutrient-injecting surface* (see Fig. 1) by the beach surface which is lower than the high tide line and higher than the tidal level by a constant Δw^* and has a unit length of 1 m in the shoreline direction. The nutrient-injecting surface extends seaward as the tide falls and withdraws landward as the tide rises. The nutrient injection begins when the tidal level falls to the elevation of high tide level $-\Delta w^*$. Given the beginning time of nutrient injection which is immediately after the high tide, to ensure

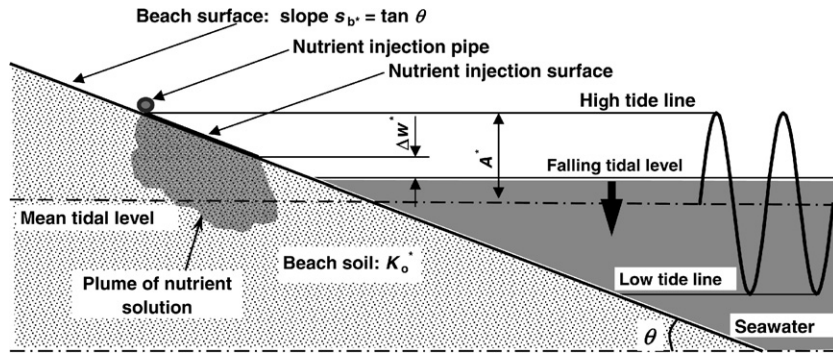


Fig. 1. Schematic of a beach cross-section vertical to the shoreline and the nutrient-injecting surface.

that there is enough nutrient in beach soils near the low tide line, the nutrient injection should at least continue to the low tide, or a little bit conservatively and conveniently, it should last for half tidal cycle. On the other hand, further injection when the tide rises is obviously a waste of the nutrient because the rising tide may wash out the nutrients immediately after they are released. So the injection duration is chosen to be half tidal cycle.

To quantify the amount of solution, we conducted a numerical investigation of the beach groundwater hydraulics and solute transport, taking into account the effects of the tidal action on beach hydraulics and the freshwater–saltwater interaction. The equations governing water flow and solute transport (salt and nutrient) were coded in a dimensionless, two-dimensional numerical model MARUN (Boufadel et al., 1999a; Boufadel, 2000) for describing the density-and-viscosity-dependent flow in a variably-saturated beach cross-section vertical to the shoreline. The model incorporated all the important and complex factors such as the seepage face, soil permeability and capillary effects, tidal amplitude and period and the beach slope.

3.1. Beach domain and tide

Fig. 2 shows the cross-section of the beach in our numerical model. Proper vertical and horizontal scaling factors were used to transform the real beach domain in Fig. 2a into the dimensionless domain in Fig. 2b which has a fixed slope of $s_b = 10\%$. The flow and solute transport equations were written in dimensionless forms and solved in the dimensionless domain. In the dimensionless model, the slope s_b appears only in the flow and solute transport governing differential equations. The numerical solutions for different beach slopes can be obtained by adjusting the s_b -value using the same dimensionless domain and mesh.

The dimensionless beach domain in Fig. 2b has a length of $L_x = 80$ and height of $L_z = 5$. The bottom is assumed to be impermeable. For a real beach area with tidal amplitude A^* [L] and beach slope s_b , letting the vertical characteristic scale be A^* and horizontal characteristic scale be A^*s_b/s_b , the dimensionless domain is transformed into different dimensional domains with vertical height $L_z^* = L_z A^* = 5A^*$

and horizontal length $L_x^* = L_x A^* s_b / s_b = 8A^*$. The characteristic time scale is defined as:

$$T_s^* = A^* / K_0 \tag{1}$$

and the fundamental transforms with respect to the spatial and temporal variables are

$$x = \frac{s_b x^*}{s_b A^*}, \quad z = \frac{z^*}{A^*}, \quad t = \frac{t^*}{T_s^*}, \tag{2}$$

where x^* and z^* are the horizontal and vertical coordinates for the dimensional domain, respectively (Fig. 2a), and x and z are the horizontal and vertical coordinates of the dimensionless domain, respectively (Fig. 2b). The term t^* is time and t is the dimensionless time. The sea tide, which is assumed to be sinusoidal with a period of T^* , is described by the following dimensionless form:

$$h_{sea}(t) \stackrel{\text{def.}}{=} h_m + \cos\left(\frac{2\pi}{T^*} t\right), \tag{3a}$$

where

$$T = \frac{T^*}{T_s^*} = \frac{T^* K_0}{A^*} \tag{3b}$$

is the dimensionless tidal period, h_m is the ratio of the mean sea level to the tidal amplitude. By setting $h_m = 3.0$, the dimensionless tidal level fluctuates between the elevations 2.0 and 4.0 (Fig. 2b).

In the numerical simulations, the nutrient solution has a nutrient concentration of 2.0 g/L and salt concentration of 32.0 g/L, a typical value of the seawater concentration. The numerical solution for an arbitrary nutrient concentration c_{inj}^* of the nutrient solution for injection can be determined proportionally from the ratio of c_{inj}^* to the value 2.0 g/L as long as c_{inj}^* is small enough (e.g., less than 5.0 g/L), because in this case the model is approximately linear with respect to the nutrient concentration in the beach.

In the dimensionless domain, the nutrient-injecting surface is the beach surface which is lower than the high tide line ($z = 4.0$) and higher than the tidal level $h_{sea}(t)$ by a constant $\Delta w^* / A^*$ and has a unit length of 1 m in the shoreline direction. The nutrient injection begins when the tidal level falls to the elevation of 3.80 (i.e., $\Delta w^* / A^* = 0.2$).

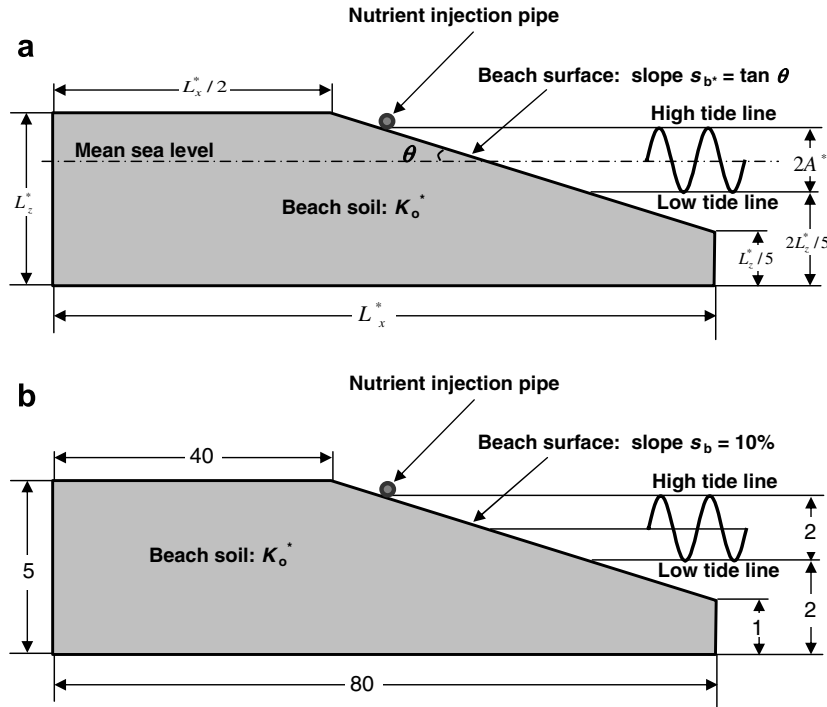


Fig. 2. Beach cross-sectional domains for (a) real dimensional and (b) dimensionless model formulations.

3.2. Dimensionless flow and transport equations

Using the transforms of the temporal and spatial variables defined in Eq. (2), the flow equation is written as the dimensionless form in the dimensionless beach domain (Li et al., submitted for publication) which is a coupled nonlinear partial differential equation including the dimensionless pressure ψ (the ratio of the pressure head to the tidal amplitude, i.e., $\psi = \psi^*/A^*$), and the total concentration $c^* = c_s^* + c_{nut}^*$ [ML^{-3}], where c_s^* and c_{nut}^* being the salt and nutrient concentrations, respectively. A typical porosity value of 0.30 was used. In the unsaturated zone, the hydraulic conductivity and the capillary pressure depend on the soil water saturation and described by a dimensionless form derived from the van Genuchten (1980) model which includes three soil parameters S_r , α^* and n . Here S_r is residual water saturation and a fixed typical value of 0.01 was used. The parameter α^* [L^{-1}] represents the characteristic pore size of the beach soil. Higher α^* values imply a coarser material. The inverse of α^* provides an estimate of the capillary fringe (zone of considerable moisture above the water table). In the dimensionless model, the parameter α^* was set to $\alpha^* = 10/A^*$. The term n represents the uniformity of the pores and higher values of n imply a more uniform pore-size distribution (van Genuchten, 1980; Wise et al., 1994b). In our numerical model, an average value $n = 3.0$ was used.

Following Zhao et al. (2006) and Li et al. (submitted for publication), the transport of the salt and nutrient (regarded as the total concentration $c^* = c_s^* + c_{nut}^*$) is also written as a dimensionless form in the dimensionless

domain with a dimensionless dispersion coefficient defined as

$$D_f = \frac{D_f^*}{A^* K_o^*} \quad (4)$$

where D_f^* [$L^2 T^{-1}$] is the velocity-independent constant dispersion coefficient. A conservative value of 0.01 was used for the parameter D_f . The transport of the nutrient component (c_{nut}^*) is described by the same dimensionless transport equation after the total concentration c^* was replaced by c_{nut}^* . Details of the dimensionless formulation of the flow and solute transport equations can be found in Li et al. (submitted for publication) and Boufadel et al. (1999a,c).

3.3. Boundary and initial conditions

On the saturated part of the left-hand side boundary, the water is fresh and the watertable is a constant (the tide-induced watertable fluctuation dies out). The inland water table sufficiently far from the coastline is significantly high than the mean sea level even in the case when there is no net inland recharge (e.g., Nielsen, 1990; Li et al., 2000; Teo et al., 2003; Li and Jiao, 2003). Here the watertable at the left boundary is set to be the high tide (4.0) to ensure adequate inland freshwater recharge. No-flow and zero dispersion flux boundary conditions were assigned on the domain bottom $\{0 \leq x < 80, z = 0\}$ and the boundaries of the unsaturated zone, which include the upper part of the left-hand side $\{x = 0, z > 4\}$, the upper surface $\{0 \leq x < 40, z = 5\}$, and the beach surface above the seepage face which varies with time due to the tidal level

fluctuations. On the saturated part of the land-sea interface, the total concentration equals the seawater concentration c_{sea}^* (a constant of 32.0 g/L), the nutrient concentration in the seawater is assumed to be always zero and the pressure head is determined by the tidal sea level. At the seepage face, both the dimensionless pressure head ψ and the dispersion flux were set to zero to simulate the “outward boundary condition” (Galeati et al., 1992; Boufadel, 2000). This boundary condition ensures that the solute leaves the domain without change in its value. Details about numerical approaches of seepage face can be found in Li et al. (submitted for publication), Boufadel et al. (1999b), Cooley (1983), Pinder and Gray (1977) and Neuman (1973).

Before running the simulations of nutrient-injection, the periodic steady state solution was calculated using the model without nutrient (i.e., $c_{\text{nut}}^* \equiv 0$ everywhere and any time). To find the periodic numerical solution without nutrient, an approximate initial condition was used. Details of the periodical numerical solutions were given in Li et al. (submitted for publication). As an example, Fig. 3a shows salinity (in kg m^{-3} , thin lines), the velocity field (arrows), degree of water saturation (fraction of the pore volume occupied by water, dotted lines), the beach water table and the sea level (thick dashed line) at high tide when $(s_b^*, T) = (0.316, 4.41)$. Fig. 3b–d are the results at falling mid-tide, low tide, and rising mid-tide, respectively. The periodical tidal submersion of the beach surface forms a salt plume beneath the intertidal zone. A clear freshwater discharge path separates the salt plume beneath the intertidal zone from that below the low tide line. The inland freshwater discharge outlet is located near the low tide line.

After obtaining the periodically steady numerical solution, the numerical simulation of the nutrient injection was conducted. As discussed in Sections 2 and 3.1, the nutrient injection begins when the dimensionless sea level falls from the high tide to 3.80, or equivalently, approximately 0.10 tidal cycles after the high tide. The salt concentration and dimensionless pressure head of the periodic numerical solution when the dimensionless sea level falls from the high tide to 3.80 were used as the initial conditions. The initial value of nutrient concentration in the domain is zero. During the nutrient-injection period \mathbf{P}_{Inj} , the boundary conditions on the nutrient-injecting surface Γ_{Inj} are

$$\psi|_{(x,z) \in \Gamma_{\text{Inj}}} = 0, \quad \text{if } t \in \mathbf{P}_{\text{Inj}}, \quad (5a)$$

$$c^*|_{(x,z) \in \Gamma_{\text{Inj}}} = 34.0 \text{ g/L}, \quad \text{if } t \in \mathbf{P}_{\text{Inj}}, \quad (5b)$$

$$c_{\text{nut}}^*|_{(x,z) \in \Gamma_{\text{Inj}}} = 2.0 \text{ g/L}, \quad \text{if } t \in \mathbf{P}_{\text{Inj}}. \quad (5c)$$

The nutrient solution for injection is obtained by adding 2.0 g nutrient into per liter seawater which has a salt concentration of $c_{\text{sea}}^* = 32.0 \text{ g/L}$. So a total concentration of 34.0 g/L is used in Eq. (5b). Before and after the nutrient injection period, the above natural infiltration boundary

conditions in (5) were replaced by the no-flow and zero dispersion flux boundary conditions.

The model was numerically solved using the MARUN code (Boufadel et al., 1999a). Details of the parameter relationships for the dimensionless and dimensional model, domain discretization, and numerical techniques for seepage face are summarized in Li et al. (submitted for publication).

4. Results

Numerical solutions were calculated for 6 cases when the beach slope $s_b^* = 0.0316, 0.1, 0.316$ and $T = 4.41$, and 44.1. Fig. 4 shows the nutrient concentration (in g/L, thin lines), degree of water saturation (fraction of the pore volume occupied by water, dotted line), the Darcy velocity field (arrows) and the water table (thick dashed line) for $(s_b^*, T) = (0.316, 4.41)$ at (a) the first low tide after beginning of the nutrient injection, (b) the first high tide, (c) the second low tide, and (d) the second high tide. Figs. 5–9 are the situations for the other 5 cases when $(s_b^*, T) = (0.316, 44.1)$, $(0.1, 4.41)$, $(0.1, 44.1)$, $(0.036, 4.41)$ and $(0.036, 44.1)$, respectively. The analyses of the nutrient concentrations and water saturations for the 6 cases lead to the following conclusions:

- (i) For beaches with slopes of 0.10 or 0.316, either the nutrient concentration in the bioremediation zone near the low tide line is lower than the effective value at the first high tide after beginning of the nutrient injection (e.g., the cases for $(s_b^*, T) = (0.316, 4.41)$ and $(0.1, 44.1)$ shown in Figs. 4 and 7), or the water saturation near the high tide line is not high enough (less than 0.3) at the second low tide after beginning of the nutrient injection (e.g., all the cases for $s_b^* = 0.10$ and 0.316 in Figs. 4–7). In these cases, we suggest that the nutrient injection should be repeated at each tidal cycle, but with smaller nutrient concentrations (e.g., 1/5 of 2.0 g/L) because the 0.002 g/L contours at the first high tide are very close to the 0.01 g/L contours. If the nutrient concentration for injection is 0.4 g/L, the 0.002 g/L contours will be located where the current contours for 0.01 g/L are. In addition, our simulations considered only one single injection period (no initial nutrient in the beach soils) and the dispersion was simulated conservatively with a small constant dispersion coefficient $D_f = 0.01$ (Li et al., submitted for publication).
- (ii) For beaches with small slope of 0.0316, the water saturation near the high tide line can reach 0.6 even at the second low tide and the nutrient concentration is still above the effective value in the bioremediation zone even at the second low and high tides (Figs. 8 and 9). In this case the nutrient injecting frequency can be reduced to once per two tidal cycles.
- (iii) The nutrient plume moves mainly seaward when the tide falls and mainly downward when the tide rises,

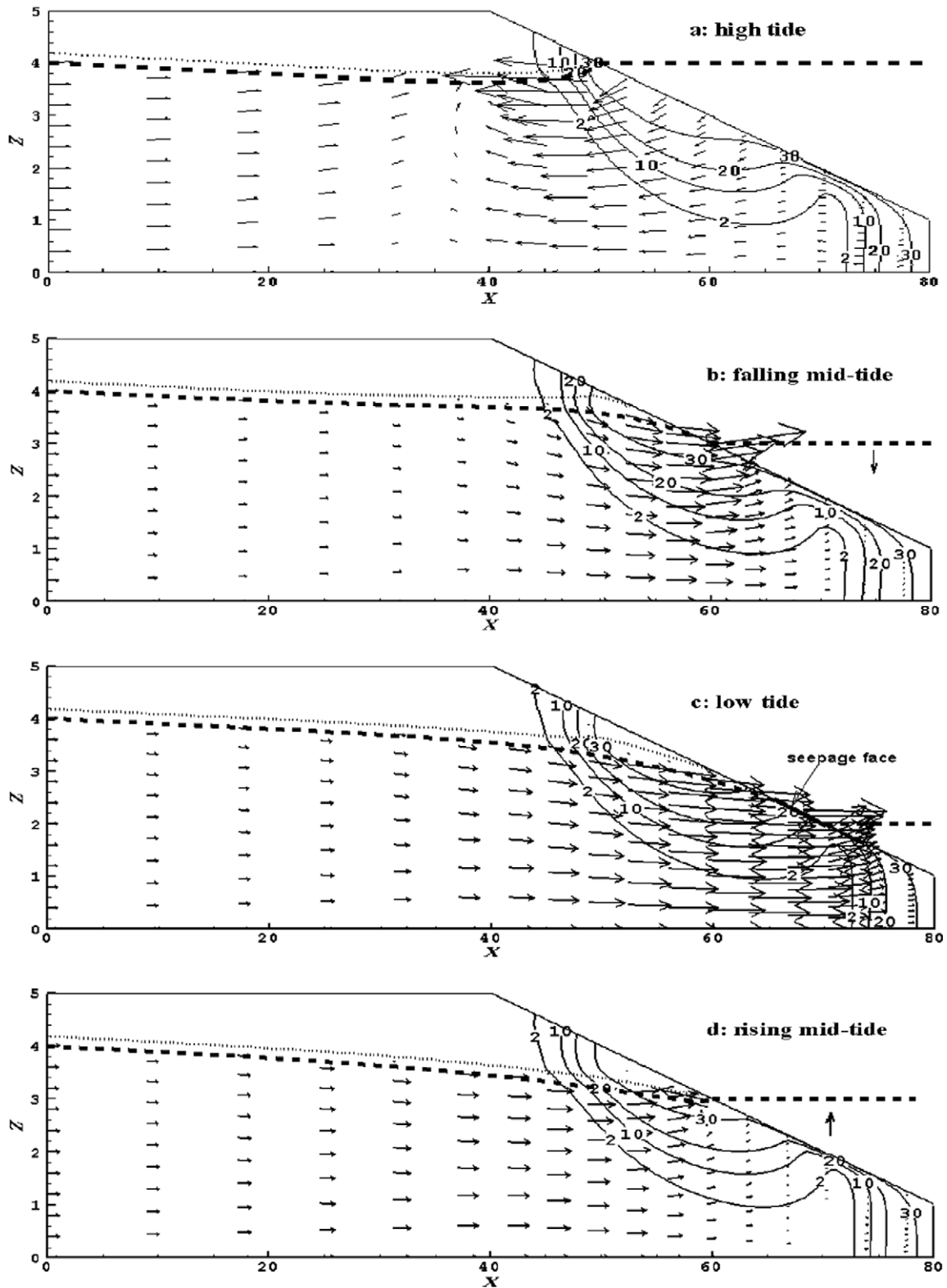


Fig. 3. Salinity (in g/L), velocity field, and degree of water saturation of the periodic numerical solution without nutrient injection for $(s_b, T) = (0.316, 4.41)$ at four different times. The thin lines represent the salinity. The arrows represent the Darcy flux. The dotted line represents the degree of water saturation of 30%. The dashed line represents the beach water table.

which is consistent with the laboratory observations of tracer studies conducted by Boufadel et al. (2006). Because the outlet of the inland freshwater discharge

path is located near the low tide line (Li et al., submitted for publication; Robinson et al., 2006, 2007), the nutrient concentration near the low tide line remains

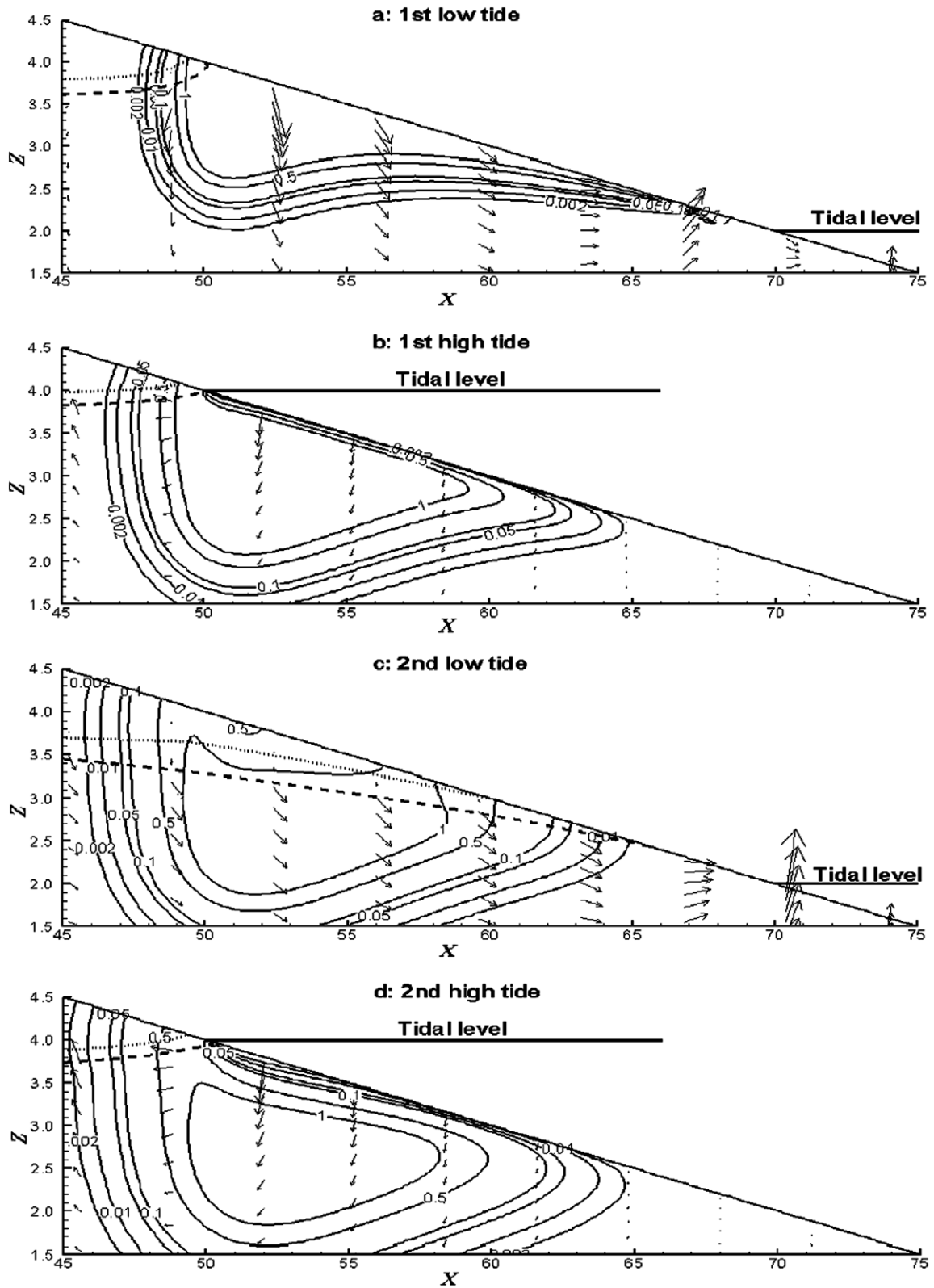


Fig. 4. Nutrient concentration (in g/L), velocity field, and degree of water saturation for $(s_b, T) = (0.316, 4.41)$ at four different times. The thin lines represent the nutrient concentration. The arrows represent the Darcy flux. The dotted line represents the degree of water saturation of 30%. The dashed line represents the beach water table.

very low until the nutrient solution infiltrates downward and mixes with the deep freshwater and then

moves along the freshwater discharge path to the outlet. This is why the nutrient concentration near

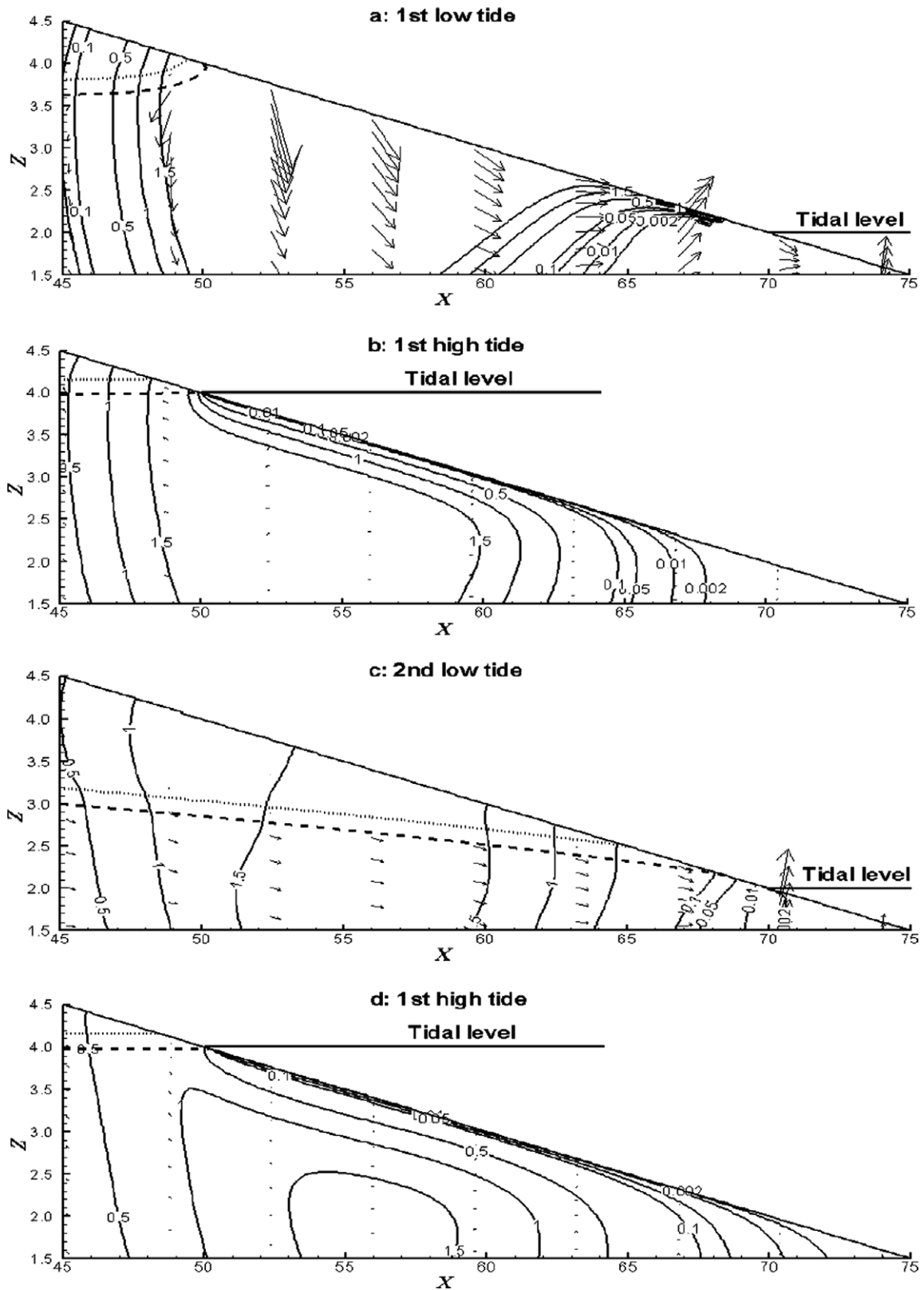


Fig. 5. Nutrient concentration (in g/L), velocity field, and degree of water saturation for $(s_b^*, T) = (0.316, 44.1)$ at four different times. The thin lines represent the nutrient concentration. The arrows represent the Darcy flux. The dotted line represents the degree of water saturation of 30%. The dashed line represents the beach water table.

the outlet is lower than the effective value for almost all cases in Figs. 4–9. There are only two exceptional cases

at the 2nd low tide in Figs. 5c and 7c, where the relatively steep beach slope of $(s_b^* = 0.316$ and $0.1)$ and

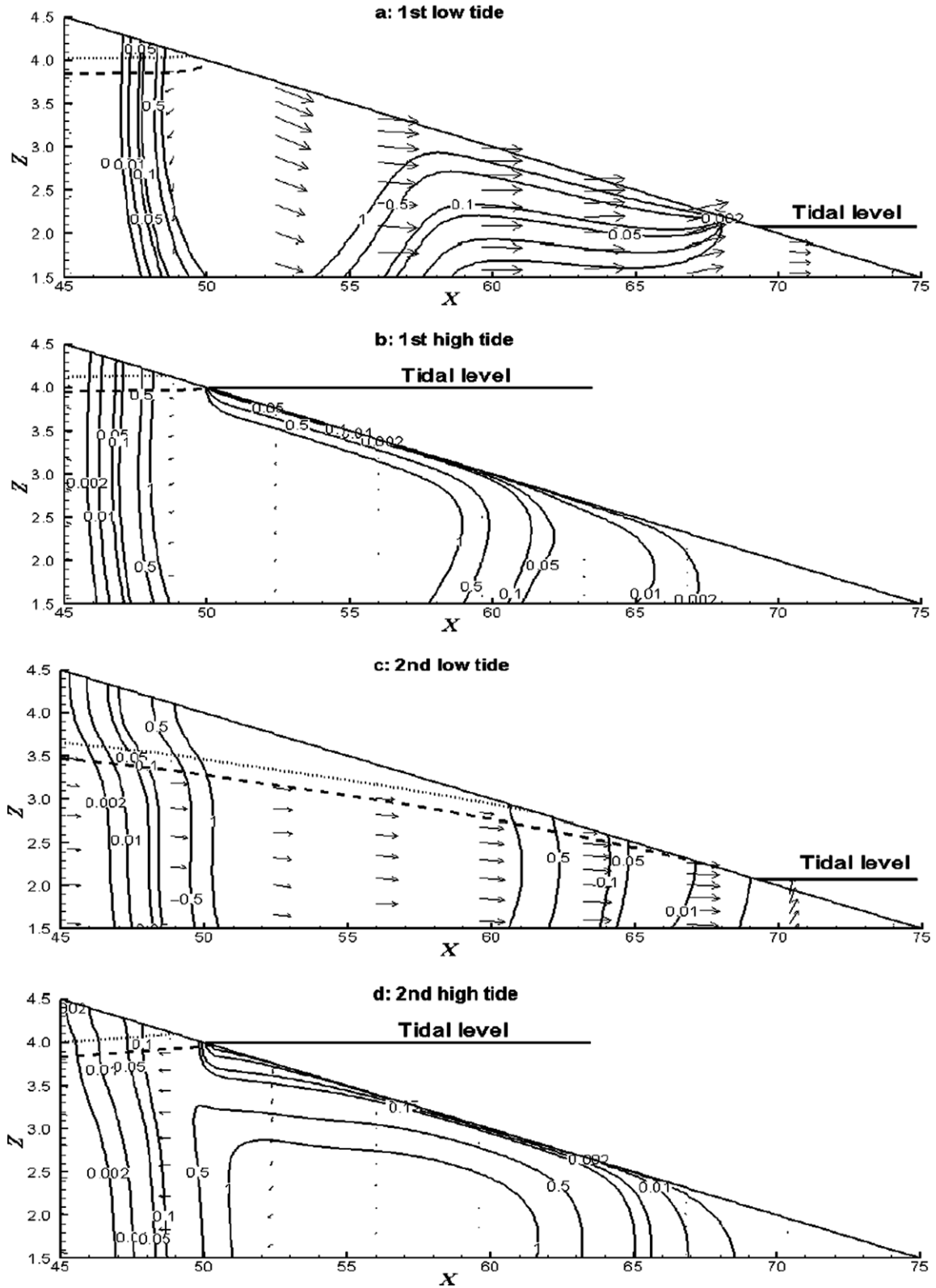


Fig. 7. Nutrient concentration (in g/L), velocity field, and degree of water saturation for $(s_b^*, T) = (0.1, 44.1)$ at four different times. The thin lines represent the nutrient concentration. The arrows represent the Darcy flux. The dotted line represents the degree of water saturation of 30%. The dashed line represents the beach water table.

the outlet. If the nutrient solution injection is conducted periodically as suggested in (i) and (ii), the

nutrient concentration near the outlet will eventually reach or exceed the effective value for all the cases.

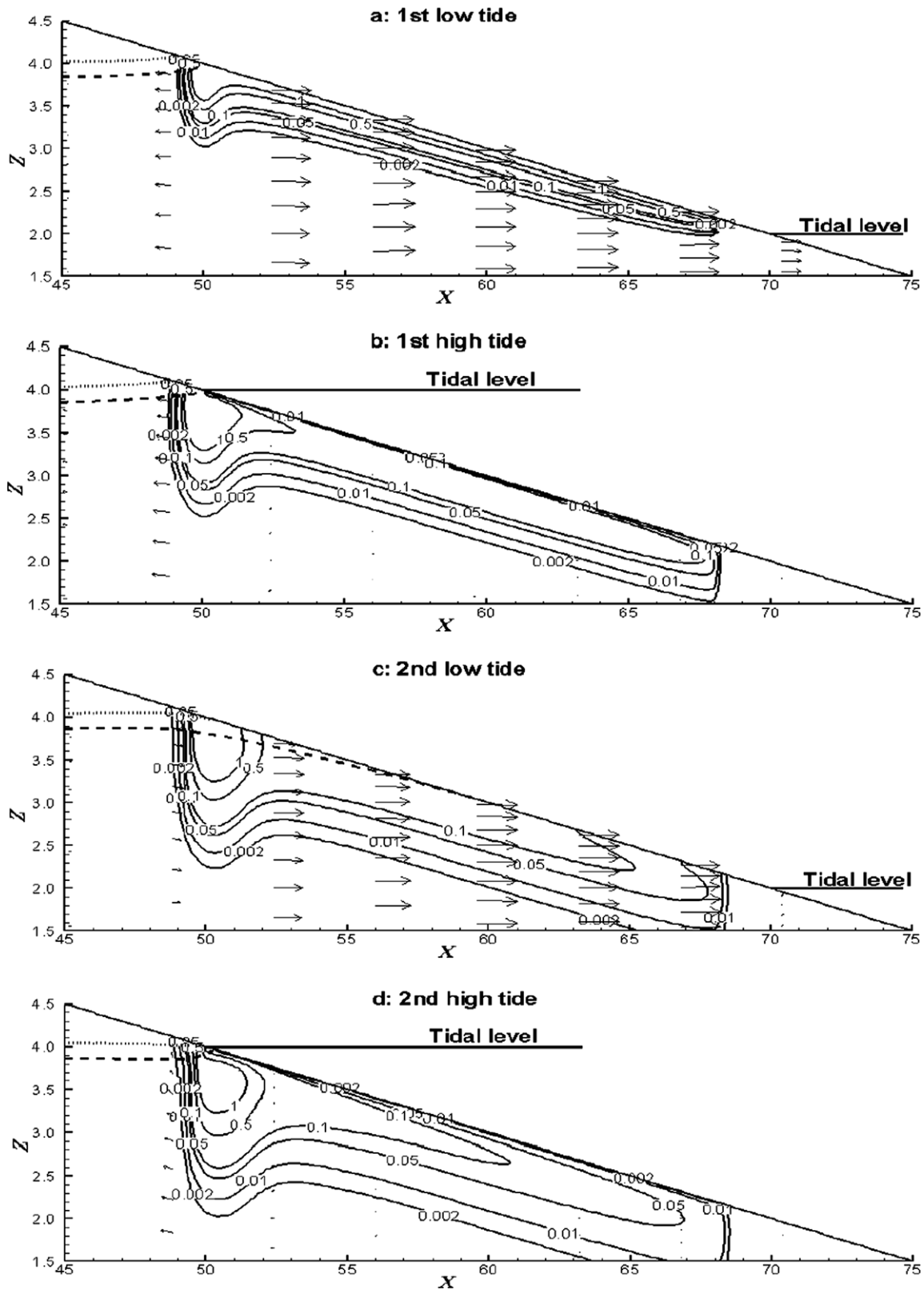


Fig. 8. Nutrient concentration (in g/L), velocity field, and degree of water saturation for $(s_b^*, T) = (0.0316, 4.41)$ at four different times. The thin lines represent the nutrient concentration. The arrows represent the Darcy flux. The dotted line represents the degree of water saturation of 30%. The dashed line represents the beach water table.

The dimensionless nutrient injection flow rate $F_{Inj}(t; s_b^*, T)$, which is defined as the ratio of the nutrient

injection flow rate to the quantity $A^*K_0^*$, was calculated for the 6 cases. The nutrient injection begins when the fall

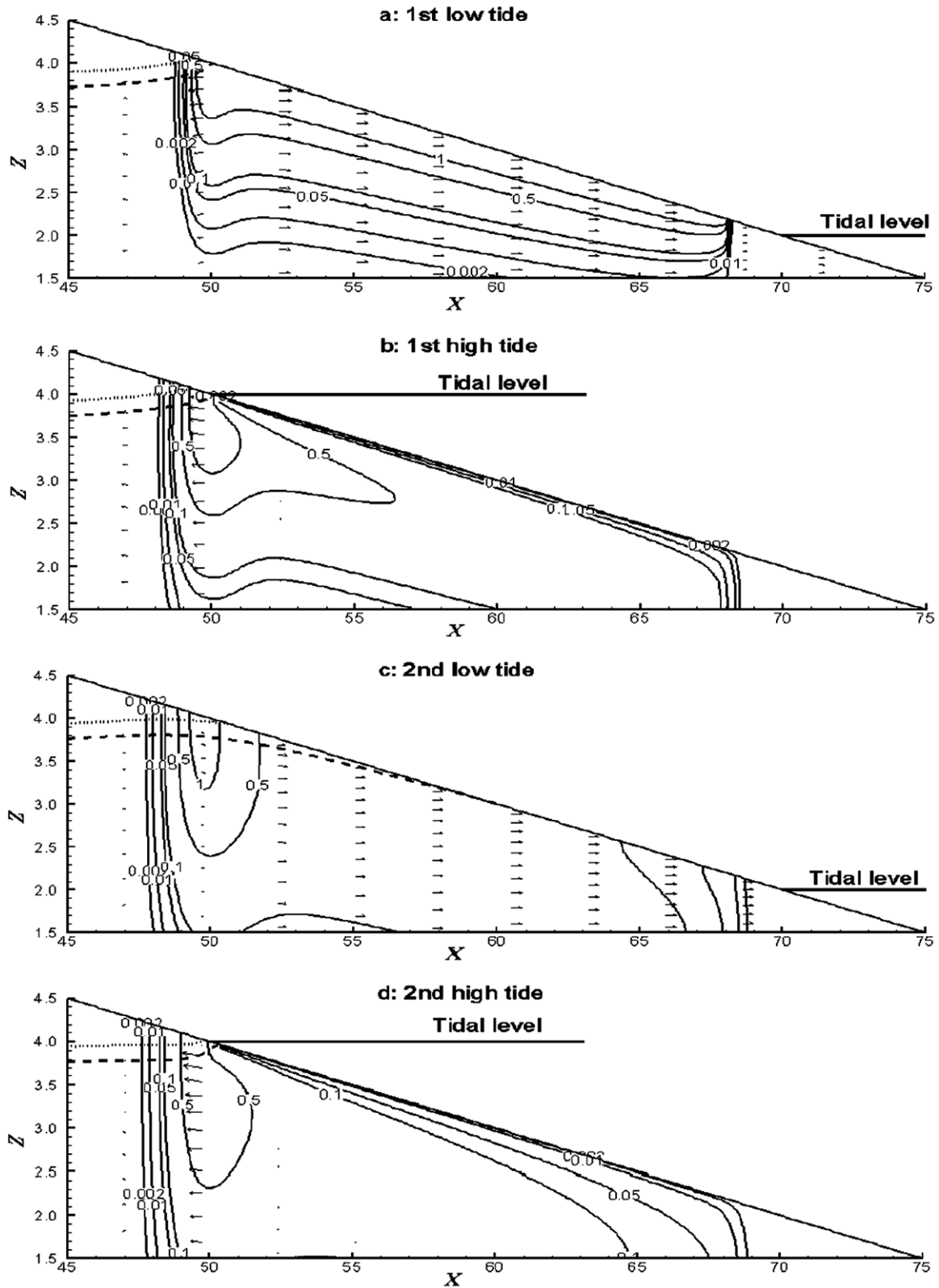


Fig. 9. Nutrient concentration (in g/L), velocity field, and degree of water saturation for $(s_b^*, T) = (0.0316, 44.1)$ at four different times. The thin lines represent the nutrient concentration. The arrows represent the Darcy flux. The dotted line represents the degree of water saturation of 30%. The dashed line represents the beach water table.

of the tidal level from the high tide reaches 20% of the tidal amplitude, or equivalently, approximately 0.10 tidal cycles

after the high tide. Fig. 10 reports it as function of time starting from an initial duration of 0.005 tidal cycles from

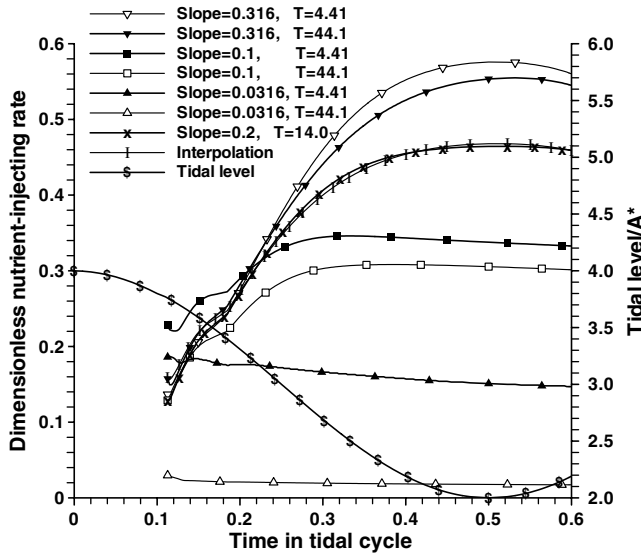


Fig. 10. Changes of the dimensionless nutrient injection flow rate $F_{inj}(t; s_b^*, T)$ with time (in tidal cycle and starting from the high tide) for different values of beach slope s_b^* and dimensionless tidal period T .

the beginning of injection. The flow values were excessively large during this initial duration of 0.005 tidal cycles due to the mathematical artifact of suddenly applying boundary conditions of zero pressure at the surface that had a negative pressure. Because the duration of these high flows was very small (only 0.005 tidal cycles), the resulting water volumes that entered the beach were also small. For this reason, it is better from an engineering point of view to omit these high flows, and to assume that the flows at the end of this initial duration existed at the beginning of injection.

The four curves for $s_b^* = 0.1$ and 0.316 abruptly become steep when the dimensionless time reaches about 0.18 (notice the “kink” in Fig. 10). Detailed analyses of the numerical solution indicated that a saturated outflowing discharge path was formed beneath the nutrient-injecting surface at this time, and a seepage face appeared on its lower part. This increased the injecting flow rate significantly and resulted in the kink. During the initial injecting stage, the four curves are very close to each other, indicating that the injecting flow rates are less sensitive to the beach slope. This is because during the initial injecting stage, the saturated outflowing discharge path was not

hydraulic conductivity. The decrease of the beach slope can reduce the drainage speed of the beach pore water as the tide falls, e.g., at the extreme case of flat beach surface, the soil becomes always saturated and no drainage happens. This explains why the dimensionless injecting flow rate decreases as the slope becomes smaller in Fig. 10. In particular, when $s_b^* = 0.0316$, the beach drainage speed is limited by the small slope so strongly that the increment of the injecting flow rate is no longer proportional to the permeability increment, as is indicated by the two curves for $s_b^* = 0.0316$ in Fig. 10. This may explain why the curve for $s_b^* = 0.0316$ and $T = 44.1$ is far below the others. In this case, although the saturated outflowing discharge path is also formed, the limited drainage speed does not enhance the dimensionless injecting flow rate significantly and so the curves have no kinks.

For greater beach slope, the constraint of the slope to the drainage speed becomes negligible and the beach hydraulic conductivity dominates the drainage speed of the beach surface. In this case, the drainage speed or the injecting flow rate will be approximately proportional to the beach hydraulic conductivity K_0^* . Consequently, the ratio of the injecting flow rate to K_0^* , or equivalently, the dimensionless injecting flow rate, should be less sensitive to the hydraulic conductivity. This may explain why the pair of curves for the same slope value $s_b^* = 0.1$ are so close to each other for different values of T , and so are those for $s_b^* = 0.316$.

5. Nomographs for practitioners

These 6 cases can be used as a set of basis for interpolation to evaluate the dimensionless nutrient injection flow rate for an arbitrary real beach system. The procedure is as follows. Given the beach slope s_b^* , hydraulic conductivity K_0^* , tidal amplitude A^* , and tidal period T^* , the dimensionless tidal period T can be determined from Eq. (3b), repeated herein for convenience:

$$T = \frac{T^* K_0^*}{A^*}. \tag{3b}$$

Then the dimensionless nutrient injection flow rate $F_{inj}(t; s_b^*, T)$ at any dimensionless time $t = \frac{t^* A^*}{K_0^*}$ is determined via interpolations with respect to the two variables (s_b^*, T) by

$$F_{inj}(t; s_b^*, T) = \frac{(p - p_1)[(\ell - \ell_1)F_{22} + (\ell_2 - \ell)F_{12}] + (p_2 - p)[(\ell - \ell_1)F_{21} + (\ell_2 - \ell)F_{11}]}{(p_2 - p_1)(\ell_2 - \ell_1)}, \tag{6}$$

formed yet and the injecting flow rate was mainly determined by the infiltration, which is independent of the beach slope.

The drainage speed of the seepage face depends on two factors: the first is the beach slope, the second is the beach

where

$$p = \lg T, \quad (p_1, p_2) = (\lg T_1, \lg T_2) = (\lg 4.41, \lg 44.1); \tag{7a}$$

$$\ell = \lg s_b^*, \quad \ell_1 = \lg s_1, \quad \ell_2 = \lg s_2, \tag{7b}$$

$$(s_1, s_2) = (0.0316, 0.1) \quad \text{if } 0.0316 < s_{b^*} \leq 0.1 \quad \text{and} \quad (7c)$$

$$(s_1, s_2) = (0.1, 0.316) \quad \text{if } 0.1 < s_{b^*} \leq 0.316; \quad (7d)$$

$$F_{ij} = F_{\text{Inj}}(t; s_i, T_j), \quad i, j = 1, 2. \quad (7e)$$

Linear interpolations with respect to the variables $\lg s_{b^*}$ and $\lg T$ are used instead of s_{b^*} and T , because several numerical tests indicated that the results of the log-based interpolation were closer to the numerical solutions. Table 1 gives the value ranges of the beach slope s_{b^*} and hydraulic conductivity K_0^* for saturated freshwater applicable for our interpolation method based on the curves from Fig. 10 when the tidal amplitude A^* ranges from 0.3 m to 2.0 m and the tidal period T^* equals 12.25 h (approximating semidiurnal tide) or 24.5 h (approximating diurnal tide).

Example: Assume a beach has the following parameter values: slope $s_{b^*} = 20\%$, permeability $K_0^* = 3.8 \times 10^{-4}$ m/s, the tidal amplitude $A^* = 1.2$ m, the tide period $T^* = 12.25$ h. Please find the nutrient injection flow rate for this beach.

Answer: Checking the row in Table 1 corresponding to $T^* = 12.25$ h, we find that $s_{b^*} = 20\%$ and $K_0^* = 3.8 \times 10^{-4}$ m/s are within their applicable value ranges, so Eqs. (6) and (7) can be used to find the nutrient injection flow rate. From definition Eq. (3b), the dimensionless tidal period is

$$T = \frac{T^* K_0^*}{A^*} = \frac{12.25 \times 3600 \times 3.8 \times 10^{-4}}{1.2} = 14.0. \quad (8)$$

Because $0.10 \leq s_{b^*} = 0.20 \leq 0.316$, setting $(s_1, s_2) = (0.10, 0.316)$ in Eq. (6), one can obtain the dimensionless nutrient injection flow rate $F_{\text{Inj}}(t; s_{b^*}, T)|_{s_{b^*}=0.20, T=14.0}$ based on the four curves in Fig. 10 corresponding to $(s_{b^*}, T) = (0.1, 4.41), (0.1, 44.1), (0.316, 4.41)$ and $(0.316, 44.1)$. We developed a Fortran code to conduct the interpolation, and the value of $F_{\text{Inj}}(t; s_{b^*}, T)|_{s_{b^*}=0.20, T=14.0}$ at each time step is reported in Fig. 10 (thin line with “I”) along with those obtained by numerically solving the governing equations of the dimensionless model (the thick line with “×”). The agreement between the curves is good indicating that the interpolation is sufficient for obtaining high accuracy. Using the values of $F_{\text{Inj}}(t; s_{b^*}, T)|_{s_{b^*}=0.20, T=14.0}$, the nutrient injection flow rate is then given by

$$\begin{aligned} F_{\text{Inj}}^*(t; s_{b^*}, T)|_{s_{b^*}=0.20, T=14.0} &= A^* K_0^* F_{\text{Inj}}(t; s_{b^*}, T)|_{s_{b^*}=0.20, T=14.0} \\ &= 4.56 \times 10^{-4} F_{\text{Inj}}(t; s_{b^*}, T)|_{s_{b^*}=0.20, T=14.0} \text{ m}^3/(\text{m s}). \end{aligned} \quad (9)$$

Table 1
Value ranges of the beach slope s_{b^*} and hydraulic conductivity K_0^* applicable for our interpolation method for usual tidal amplitude A^* and tidal period T^*

A^* (m)	T^* (h)	K_0^* (m/s)	s_{b^*}
0.3–2.0	12.25 (semidiurnal)	3×10^{-5} – 2×10^{-3}	3.16–31.6%
0.3–2.0	24.5 (diurnal)	1.5×10^{-5} – 10^{-3}	3.16–31.6%

6. Conclusions

Biostimulation via application of nutrients such as nitrogen and phosphorus is a viable technology for restoration of oil-contaminated beaches. Although the nutrient concentrations sufficient for near-maximum growth of hydrocarbon-degrading microorganisms are very small (only 2.0–10.0 mg/L), the effectiveness of biostimulation requires continuous contact between the added nutrients and the oil within the bioremediation zone. Maximizing the residence time of nutrients in this zone is the key to achieve rapid and cost-effective cleanup. We considered the situation where the nutrient solution is released through a perforated pipe at the high tide line parallel to the shoreline. The optimal nutrient application flow was obtained as result of numerical investigations of the beach groundwater hydraulics and solute transport, taking into account the effects of the tidal action, saltwater wedge, and density gradients.

Proper vertical and horizontal scaling factors were used to transform the beach domain into a dimensionless domain with a fixed slope, the flow and solute transport equations were written in dimensionless forms and solved in the dimensionless domain. The numerical solutions for different beach slopes were obtained by adjusting the s_{b^*} -value using the same dimensionless domain and mesh. A novel dimensionless, two-dimensional model MARUN (Boufadel et al., 1999a) was used to describe the density- and viscosity-dependent flows in cross-sections of variably-saturated homogeneous beaches vertical to the shorelines. The model incorporated all the important and complex factors such as the seepage face, soil permeability and capillary effects, tidal amplitude and period, and the beach slope.

Based on the analyses of the numerical simulations, the optimal nutrient application strategy was obtained. The application of the nutrient solution should begin following the high tide and should last for half a tidal cycle. The flow rate of the nutrient solution given in Fig. 10 ensures that the saturated wet-front of the nutrient solution in the beach surface moves seaward with the same speed of the falling tide keeping a constant distance from the tide line. The nutrient flow rates satisfying these optimal conditions were numerically calculated for 6 cases of the dimensionless model.

For an arbitrary tidal beach system, the optimal nutrient flow rate can be interpolated among those of the given 6 cases provided the beach slope is between 0.03 and 0.33, the beach hydraulic conductivity is between $(10^{-5}$ and 10^{-3} m/s), the tidal amplitude is between 0.3 m and 2 m and the period is either semidiurnal or diurnal. The proper interpolation is not linear, and is reported by Eq. (6). Extrapolation should be conducted with caution. The authors have written a Fortran code to conduct the interpolation, and bioremediation practitioners may obtain it from the authors at no cost.

Acknowledgements

Funding for this work was provided by the United States Environmental Protection Agency. However, no official endorsement should be inferred.

Appendix 1

List of notations

- A^* [L] tidal amplitude.
 c^* [ML^{-3}] total concentration of the beach pore water ($c^* = c_s^* + c_{\text{nut}}^*$).
 c_{nut}^* [ML^{-3}] nutrient concentration of the beach pore water.
 c_s^* [ML^{-3}] salt concentration of the beach pore water.
 c_{sea}^* [ML^{-3}] salt concentration of the seawater (=32.0 g/L).
 D_f^* [L^2T^{-1}] & D_f [-] dimensional and dimensionless dispersion coefficients, respectively.
 $F_{\text{Inj}}(t; s_b^*, T)$ [-] the dimensionless nutrient injection flow rate defined as the ratio of the *nutrient injection flow rate* to the quantity $A^*K_0^*$.
 $F_{\text{Inj}}^*(t; s_b^*, T)$ [L^2T^{-1}] the nutrient injection flow rate (the volume of nutrient solution needed in unit time and in unit length in the shoreline direction).
 $F_{\text{Inj}}^*(t; s_b^*, T) = A^*K_0^*F_{\text{Inj}}(t; s_b^*, T)$
 h_m ratio of the mean sea level to the tidal amplitude.
 h_{sea} dimensionless sea level (ratio of the sea level to the tidal amplitude).
 K_0^* [LT^{-1}] saturated freshwater hydraulic conductivity of beach soil.
 L_x^* [L] & L_x [-] horizontal lengths of the dimensional and dimensionless domains, respectively.
 L_z^* [L] & L_z [-] heights of the dimensional and dimensionless domains, respectively.
 n [-] soil parameter of the [van Genuchten \(1980\)](#) model.
 S_r [-] residual soil water saturation.
 s_b^* [-] & s_b [-] beach slopes of the dimensional and dimensionless domains, respectively.
 T^* [T] & T [-] dimensional and dimensionless tidal periods, respectively.
 T_S^* [T] the characteristic time scale, $T_S^* = A^*/K_0^*$.
 t^* [T] & t [-] dimensional and dimensionless time variables, respectively.
 x^* [L] & x [-] dimensional and dimensionless horizontal coordinates, respectively.
 z^* [L] & z [-] dimensional and dimensionless vertical coordinates, respectively.
 α^* [L] parameter of the [van Genuchten \(1980\)](#) model for describing the soil capillary effect.
 Δw^* [L] the vertical distance from the saturated wet-front of the nutrient solution to the tidal sea level (equals $0.20A^*$ in the numerical simulation).
 ψ^* [L] & ψ [-] dimensional and dimensionless pressure heads, respectively.

References

- Asservatham, A.M., Kang, H.Y., Nielsen, P., 1993. Groundwater movement in beach watertables. In: 11th Australasian Conference on Coastal and Ocean Engineering IE Australia. Crows Nest, NSW, Australia 2, pp. 589–594.
- Boufadel, M.C., 1998. The transport of nutrients in beaches: effect of tides, waves, and buoyancy, Department of Civil and Environmental Engineering, Cincinnati, Ohio, University of Cincinnati, PhD Dissertation, p. 413.
- Boufadel, M.C., 2000. A mechanistic study of nonlinear solute transport in a groundwater-surface water system under steady state and transient hydraulic conditions. *Water Resour. Res.* 36, 2549–2565.
- Boufadel, M.C., Suidan, M.T., Venosa, A.D., 1999a. A numerical model for density-and-viscosity-dependent flows in two-dimensional variably-saturated porous media. *J. Contam. Hydrol.* 37, 1–20.
- Boufadel, M.C., Suidan, M.T., Venosa, A.D., Bowers, M.T., 1999b. Steady seepage in trenches and dams: effect of capillary flow. *J. Hydraul. Eng. ASCE* 125, 286–294.
- Boufadel, M.C., Suidan, M.T., Venosa, A.D., 1999c. Numerical modeling of water flow below dry salt lakes: effect of capillarity and viscosity. *J. Hydrol.* 221, 55–74.
- Boufadel, M.C., Reeser, P., Suidan, M.T., Wrenn, B.A., Cheng, J., Du, X., Venosa, A.D., 1999d. Optimal nitrate concentration for the biodegradation of *n*-heptadecane in a variably-saturated sand column. *Environ. Technol.* 20, 191–199.
- Boufadel, M.C., Suidan, M.T., Venosa, A.D., 2006. Tracer studies in laboratory beach simulating tidal influences. *J. Environ. Eng.* 132 (6), 616–623, doi:10.1061/(ASCE)0733-9372.
- Boufadel, M.C., Li, H.L., Suidan, M.T., Venosa, A.D., in press. Tracer Studies in Laboratory Beach Subjected to Waves. *J. Environ. Eng. ASCE*.
- Cooley, R.L., 1983. Some new procedures for numerical solution of variably saturated flow problems. *Water Resour. Res.* 19, 1271–1285.
- Galeati, G., Gambolati, G., Neuman, S.P., 1992. Coupled and partially coupled Eulerian-Lagrangian model of freshwater-seawater mixing. *Water Resour. Res.* 28 (1), 149–165.
- Li, H.L., Jiao, J.J., 2003. Influence of the tide on the mean watertable in an unconfined, anisotropic, inhomogeneous coastal aquifer. *Adv. Water Resour.* 26 (1), 9–16.
- Li, H.L., Zhao, Q.H., Boufadel, M.C., Venosa, A.D., submitted for publication. Freshwater-saltwater interaction in tidally influenced beaches.
- Li, L., Barry, D.A., Stagnitti, F., Parlange, J.-Y., Jeng, D.-S., 2000. Beach water table fluctuations due to spring-neap tides: moving boundary effects. *Adv. Water Res.* 23 (8), 17–24.
- Merlin, F.-X., Chaumery, C., Oudot, J., Swannell, R.P.J., Basseres, A., Dalmazzone, C., Ducreux, J., Lee, K., Reilly, T., 1995. Bioremediation: results of the field trials of Landevennec (France). In: Proceedings of the International Oil Spill Conferences, American Petroleum Institute, Washington, DC, pp. 917–918.
- Millham, N.P., Howes, B.L., 1994. Nutrient balance of a shallow coastal embayment: 1. Patterns of groundwater discharge, *Marine ecology progress series*. Oldendorf 112 (1–2), 155–167.
- Neuman, S.P., 1973. Saturated-unsaturated seepage by finite elements. *J. Hydra. Div. ASCE* HY12, 2233–2250.
- Nielsen, P., 1990. Tidal dynamics of the watertable in beaches. *Water Resour. Res.* 26 (9), 2127–2134.
- Pinder, G.F., Gray, W.G., 1977. Finite Element Simulation in Surface and Subsurface Hydrology. Academic Press, New York, p. 294.
- Portnoy, J.W., Nowicki, B.L., Roman, C.T., Urish, D.W., 1998. The discharge of nitrate-contaminated groundwater from developed shoreline to marsh-fringed estuary. *Water Resour. Res.* 34 (11), 3095–3104, 98WR02167.
- Robinson, M.A., Gallagher, D.L., 1999. Model of ground water discharge from an unconfined coastal aquifer. *Ground Water.* 37 (1), 80–87.

- Robinson, C., Gibbes, B., Li, L., 2006. Driving mechanisms for groundwater flow and salt transport in a subterranean estuary, *Geophys. Res. Lett.* 33, L03402. doi:10.1029/2005GL025247.
- Robinson, C., Li, L., Barry, D., 2007. Effect of tidal forcing on a subterranean estuary. *Adv. Water Resour.* 30, 851–865. doi:10.1016/j.advwatres.2006.07.006.
- Teo, H.T., Jeng, D.S., Seymour, B.R., Barry, D.A., Li, L., 2003. A new analytical solution for water table fluctuations in coastal aquifers with sloping beaches. *Adv. Water Resour.* 26, 1239–1247.
- Uchiyama, Y., Nadaoka, K., Roelke, P., Adachi, K., Yagi, H., 2000. Submarine groundwater discharge into the sea and associated nutrient transport in a sandy beach. *Water Resour. Res.* 36 (6), 1467–1479, doi:10.1029/2000WR900029.
- van Genuchten, M.T., 1980. A closed-form equation for predicting the hydraulic conductivity of unsaturated soils. *Soil Sci. Soc. Am. J.* 44, 892–898.
- Venosa, A.D., Suidan, M.T., Wrenn, B.A., Strohmeier, K.L., Haines, J., Eberhart, B.L., King, D., Holder, E., 1996. Bioremediation of an experimental oil spill on the shoreline of Delaware Bay. *Environ. Sci. Technol.* 30, 1764–1775.
- Wise, W.B., Guven, O., Molz, F.J., McCutcheon, S.C., 1994a. Nutrient retention time in high-permeability, oil-fouled beach. *J. Environ. Eng. ASCE* (120), 1361–1379.
- Wise, W.R., Clement, T.P., Molz, F.J., 1994b. Variably saturated modeling of transient drainage: sensitivity to soil properties. *J. Hydrol.* 161, 91–108.
- Wrenn, B.A., Boufadel, M.C., Suidan, M.T., Venosa, A.D., 1997. Nutrient transport during bioremediation of crude oil contaminated beaches. In: *Fourth International Symposium on In-situ and On-site Bioremediation*, vol. 4. Batelle Press, New Orleans, LA, pp. 267–272.
- Wrenn, B.A., Sarnecki, K.L., Kohar, E.S., Lee, K., Venosa, A.D., 2006. Effects of nutrient source and supply on crude oil biodegradation in continuous-flow beach microcosms. *J. Environ. Eng. ASCE* 132, 75–84.
- Zhao, Q.H., Li, H.L., Ibrahim, I., Boufadel, M.C., 2006. Transport of solute plumes in beaches, In: *7th International Conference on Hydrosience and Engineering (ICHE-2006)*, Philadelphia, USA, September, 2006.